Towards the 3D Modelling of the Effective Conductivity of Solid Oxide Fuel Cell Electrodes – Validation against experimental measurements and prediction of electrochemical performance

K. Rhazaoui[1], Q. Cai[2], M. Kishimoto[1], F. Tariq[1], M. R. Somalu[3], C. S. Adjiman[4], N. P. Brandon[1]

[1] Department of Earth Science and Engineering, Imperial College London, London, SW7 2AZ, UK

[2] Department of Chemical and Process Engineering, University of Surrey, Guilford, GU2 7XH, UK

[3] Fuel Cell Institute, Universiti Kebangsaan Malaysia, 43600 UKM Bangi, Selangor, Malaysia

[4] Department of Chemical Engineering, Centre for Process Systems Engineering, Imperial College London, London, SW7 2AZ, UK

Corresponding author: N. Brandon

Email: n.brandon@imperial.ac.uk

Telephone: +442075947470

Abstract

The effective conductivity of thick-film solid oxide fuel cell (SOFC) electrodes plays a key role in their performance. It determines the ability of the electrode to transport charge to/from reaction sites to the current collector and electrolyte. In this paper, the validity of the recently proposed 3D resistor network model for the prediction of effective conductivity, the ResNet

model, is investigated by comparison to experimental data. The 3D microstructures of Ni/10ScSZ anodes are reconstructed using tomography through the focused ion beam and scanning electron microscopy (FIB-SEM) technique. This is used as geometric input to the ResNet model to predict the effective conductivities, which are then compared against the experimentally measured values on the same electrodes. Good agreement is observed, supporting the validity of the ResNet model for predicting the effective conductivity of SOFC electrodes. The ResNet model is then combined with the volume-of-fluid (VOF) method to integrate the description of the local conductivity (electronic and ionic) in the prediction of electrochemical performance. The results show that the electrochemical performance is in particular sensitive to the ionic conductivity of the electrode microstructure, highlighting the importance of an accurate description of the local ionic conductivity .

Keywords: solid oxide fuel cell, 3D, effective conductivity, resistor network,

1. Introduction

Solid oxide fuel cells (SOFCs) are high-efficiency energy conversion devices capable of operation on a wide range of fuels. SOFCs comprise a cathode, an anode, and a dense ceramic oxide ion conducting electrolyte. The electrodes have a porous and tortuous microstructure, within which electrochemical reactions take place at the meeting points of the ionic, electronic and gas phases, termed triple phase boundaries (TPBs). These TPBs have to be established by contact between percolated phases through which chemical species can be effectively transported to and from the TPBs. Alongside the requirement for fuels and products to be transported easily in the electrode pore space, there is also a need to provide a

2

large TPB length in the electrode, as well as a large number of pathways for the transport of charge carriers in the solid phases. However, the number and lengths of the transport pathways is not sufficient to fully characterize an electrode microstructure; a comprehensive understanding of the percolated solid and pore networks is required, which can only be achieved by studying the three-dimensional (3D) microstructure. The capability to model the transport and electrochemical processes in these porous composites provides a link between the electrode performance and the underlying microstructure, and thus the design of electrodes with desirable microstructure.

Structural properties such as porosity, tortuosity factor and effective conductivity of SOFC electrodes have been used as performance indicators, and indeed provide a quantitative basis for a better understanding of highly heterogeneous microstructures. Of particular interest is the effective conductivity which is related to the electronic and ionic transport processes, and correlates strongly with the electrochemical performance of the electrodes. There have been growing efforts in developing models to predict the effective conductivities of SOFC electrodes because they can provide insights into the physics behind the measured conductivity, they can help to analyse the effects of microstructure change on conductivity over time, and support electrode design studies, for example using synthetically generated structures, to explore the effect of a wide range of microstructures on conductivity, and electrochemical performance. One of the approaches proposed to date is based on percolation theory and the simulation of the electrode as a random mixture of electronic and ionic conducting particles [1-3]. The approach depends upon an arbitrary coordination number (the number of contacts a particular particle makes with its neighbouring particles) and primary parameters such as particle radii, volumetric packing density and porosity. Resistor network models [4-7] have also been used to simulate the electrodes as resistor networks and derive

the effective conductivities by applying Kirchhoff's current conservation law to the equivalent electronic circuits. The resistor network is often drawn from randomly packed electronic and ionic spherical particles in which one particle is essentially represented by one vertex in the resistor network, and each vertex is assigned a resistance to represent a particular phase in an SOFC electrode. Recently, the 3D imaging of experimental SOFC electrode microstructures has been made possible through focused ion beam-scanning electron microscope (FIB-SEM) or X-ray computed tomography (XCT) techniques [8-14, 36]. This has in turn further promoted the development of modeling methods to derive effective conductivities based on complex real 3D microstructures. Examples of these include the lattice Boltzmann method (LBM) [9], finite-volume-based methods such as computational fluid dynamics (CFD) [13], and finite-element-based approaches such as COMSOL multiphysics [14]. These approaches have been used to investigate the effects of microstructural properties such as particle size and porosity on effective conductivities. However, in all the studies mentioned above, the computed effective conductivities were not validated against experimentally measured values.

The porous 3D microstructure of electrodes has been investigated in several modelling frameworks to predict electrochemical performance. Suzue et al. [15] used the LBM to model the transport phenomena and electrochemical reactions in 3D SOFC anode microstructures derived using stochastic correlation reconstruction, through which 3D distributions of potential and current were obtained. Gas diffusion was assumed to be due to the combination of binary Fickian diffusion of H_2 and H_2O and Knudsen diffusion, and the Butler–Volmer equation was used to describe the charge-transfer kinetics. Shikazono *et al*. [9] used LBM simulation of the anode overpotential in a 3D microstructure reconstructed by FIB-SEM. Kishimoto *et al.* developed a 3D simulation model based on the finite volume method

combined with a sub-grid scale model which allows 3D overpotential analysis with a relatively coarse grid system [16, 17]. Lynch *et al*. [14] developed a modelling framework based on COMSOL multiphysics to predict electrochemical performance including overpotential vs current density, area specific resistance (ASR) and impedance behavior for a 3D reconstructed microstructure using X-ray nanotomography.

Golbert *et al*. [18] used the volume-of-fluid (VOF) method to analyze 3D SOFC electrode microstructures and model the transport of electronic, ionic and gas phase species, as well as electrochemical reactions. The VOF method presents the advantages of being able to handle large microstructures and to solve the transport and reaction equations efficiently. This modeling framework has provided a platform to link electrode design parameters to microstructural properties and the electrochemical performance of the electrodes. The structure in question is discretized into small cubic elements called voxels, followed by an aggregation of these voxels into discrete volumes called VOF elements. Each VOF element contains volume fractions of the pore phase, the electronic and ionic conducting phases; a VOF element in which any single phase fraction lies between 0 and 1 contains a phase interface. This methodology can capture interface information through discrete volume data and enable the representation of complex multiphase structures alongside continuous phases , which are well-suited for modelling conduction/diffusion and reaction. In applications of the VOF approach to date [18-21], the relevant conductivities have been approximated by assuming uniformity of the microstructure within each VOF element. The conductivities of the materials within one VOF element were simply calculated by multiplying the conductivity of the pure material with its volume fraction in the VOF element. This approximation does not take into account local percolation limitations and the structural complexity within a given VOF element, raising concerns about model accuracy, especially

close to the percolation threshold. We therefore improve the quality of the simulations by computing the effective conductivity of VOF elements.

A 3D effective conductivity model [22] has been developed separately to calculate the effective electronic and ionic conductivities of the microstructure (the entire electrode or the local VOF elements). The model is based on the resistor network approach (hereafter termed ResNet model). The methodology for analyzing a given structure can be summarized as follows: the 3D microstructure (real or synthetic) is initially discretized into small cubic elements (voxels), based on which a mixed resistor network is drawn. A potential difference is then applied to this network, the application of Kirchhoff's law of current conservation on the resistor network yields the corresponding currents entering and leaving the system, allowing for the equivalent resistance and hence conductivity of the entire structure to be determined. The model is simple and enables the integration of the conductivity model with a wide array of models and structures. In our previous work, the ResNet model was first validated against simple structures from which analytical effective conductivities could be extracted [22]. The model was also validated against more complex synthetic structures in a second paper [23], and was used to compute the effective conductivity of a Ni/10ScSZ reconstructed anode with a nickel content of 30% in the solid phase. It was shown that one needs to consider a sample large enough to be representative of each dimension for a meaningful analysis [23].

The primary objective of this paper is to validate the ResNet model by comparing the calculated electronic conductivities of regions of actual electrode structures measured using FIB-SEM techniques, with the measured electronic conductivities of the same electrodes. In order to ensure the reliability of the results, we first investigate in Section 2 the sample size

6

required for the microstructure to be considered representative of an entire electrode for the purpose of calculating the effective conductivity. In Section 3, we describe the fabrication, characterization and imaging of several Ni/10ScSZ electrodes. In Section 4, the measured effective conductivities of some of these anodes are compared to those computed based on the reconstructed 3D microstructures of the same anodes. The effective conductivities of a set of synthetic anodes are also computed. This provides an opportunity to test the validity of the model and to analyze the variation of the effective electronic conductivity across the percolation threshold. With a view to assess the impact of errors in the electronic conductivities on the validity of the prediction of electrochemical performance of SOFC anodes, the ResNet model is then integrated with the VOF model of Golbert et al. [18].

2. Representative sample size for investigating the effective conductivity

In order to make a valid comparison between the predicted and experimentally measured effective conductivities, it is necessary to ensure that the reconstructed 3D microstructure is large enough to represent the whole electrode. Indeed, Iwai *et al.* [24] and Shearing *et al.* [25] reconstructed 3D microstructures from FIB-SEM characterization of SOFC anodes and reported variations in the volume fractions of Ni and YSZ of up to 200% for samples from the same electrode, implying the need for a sample size of more than 10 μm^3 to ensure that the sample was representative of the entire electrode. The representative sample size was established by Shearing et al. to be 10 μm^3 for the microstructure they considered, though this is not necessarily applicable to anodes of different compositions or particle size distributions. Cai *et al.* [20] investigated, using computer-generated synthetic electrodes, the sample size required for the microstructure to be considered representative of an entire electrode. They reported that, to obtain reliable TPBs density, if the representative sample is a cube with length L related to the diameter of the packing particles, D then L/D $\geq$ 7.5 to obtain

representative results. Choi *et al.* [26] worked on the finite volume method using different types of grids to compute the effective transport properties of SOFC anodes. Their results were compared to those calculated with random walk simulations for the case of a body-centred cubic lattice of spheres, and showed that for reliable effective transport properties to be achieved, one needs to consider a domain size of at least ten times the mean particle diameter in each direction (i.e, L/D≥ 10).

In this section, the representative sample size needed to determine the effective electronic conductivity is investigated for the ResNet model. To investigate the effect of domain size on effective electronic conductivity, a series of microstructures were generated within cubes of increasing length (L), for a specific particle diameter (D) of 1 μm, hence increasing the ratio of L/D. In order to ensure that no other factor than the variation of domain size was responsible for the behavior of the effective electronic conductivity, particles were generated with a uniform size. Synthetic microstructures were generated by initially packing a cube domain with spheres using a Monte-Carlo process. The spheres represent electronically conductive particles, ionically conductive particles, and "pore former" particles. After packing, pore former particles were removed and the particles were uniformly enlarged by a factor of 1.2 to emulate sintering [20, 21]. For all the microstructures generated with a given domain size, the microstructures had, on average, a 43.5 vol% nickel, 35 vol% YSZ and 21.5 vol% porosity. However, the specific composition of each structure can vary, especially in the case of smaller domain sizes. Following the microstructure generation, the structures were discretized into voxels by adopting the discretization resolution established in previous work [23] and by Cai *et al.* [20], i.e., 20 voxels per particle diameter. The discretized microstructures were then input into the ResNet model to obtain the effective conductivities. Due to the Monte-Carlo process used to generate the structures, families of up to 300 structures were generated to obtain statistically reliable results. As the L/D ratio of the

8

structures increased, the number of structures required for statistically reliable results decreased (defined as the point where standard deviations fall below 10% of the ensemble mean average), with the highest L/D ratio considered requiring the generation of only 30 structures.
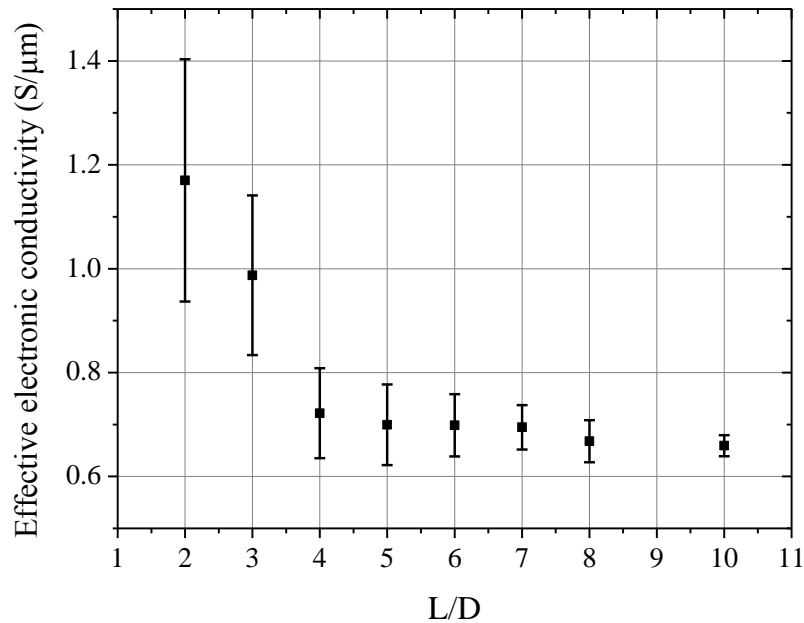

Figure 1 – Effective electronic conductivity (mean and standard deviation) as a function of L/D for families of structures with average composition given by 43.5 vol% Ni, 35 vol% YSZ and 21.5 vol% porosity, with particles of diameter 1 μm.

Figure 1 shows the mean value and standard deviation of the effective electronic conductivities of these structures in an arbitrarily chosen direction, as given by the ResNet model. As can be seen, the effective electronic conductivity data shows significant variation at low L/D ratio, and a tendency to converge at higher L/D ratios. A convergence criterion is thus set to reflect this: the first point at which the effective electronic conductivity comes within less than 5% of the previous data point is considered as the point where the whole data

set has converged. From this analysis, it can be concluded that the optimum L/D ratio to be considered for a microstructure to be representative of an entire anode, when considering effective electronic conductivity, is L/D = 8.

In Figure 1, the standard deviation (shown using error bars) is seen to decrease with an increasing domain size. The decrease in standard deviation can be attributed to the Monte-Carlo process used in generating the microstructures. For smaller packing "boxes", as few as 8-10 spheres can fill the entire domain. As the particles are randomly generated, in some cases every single sphere can represent nickel particles. It is indeed less likely for the generation to achieve the same volume fraction content in each generated structure and therefore deviations in electronic phase volume contents are more important, yielding larger variations in effective electronic conductivity, which result in the larger standard deviations observed at smaller L/D ratios. This is consistent with what might be expected in an experimental situation where, if a very small sample is taken, the sample composition may not be representative of the average composition of the structure.

Figure 1 also shows a gradual decrease of effective electronic conductivity, starting at an average value of 1.19 S/μm at L/D = 2, to a converged value of 0.63 S/μm at L/D = 10. The reason for this can be related to the variability in composition: at smaller microstructure sizes, due to the Monte-Carlo packing process described above, the entire domain can be filled with Ni particles, especially as these are most abundant particles at the chosen composition. This leads to a high effective electronic conductivity which in turn raises the average value for the family of structures. The high deviation of effective conductivities observed in Figure 1 at low L/D ratios provides evidence of this. Further evidence is given by Figure 2 which illustrates the standard deviation of Nickel content for varying L/D ratios.
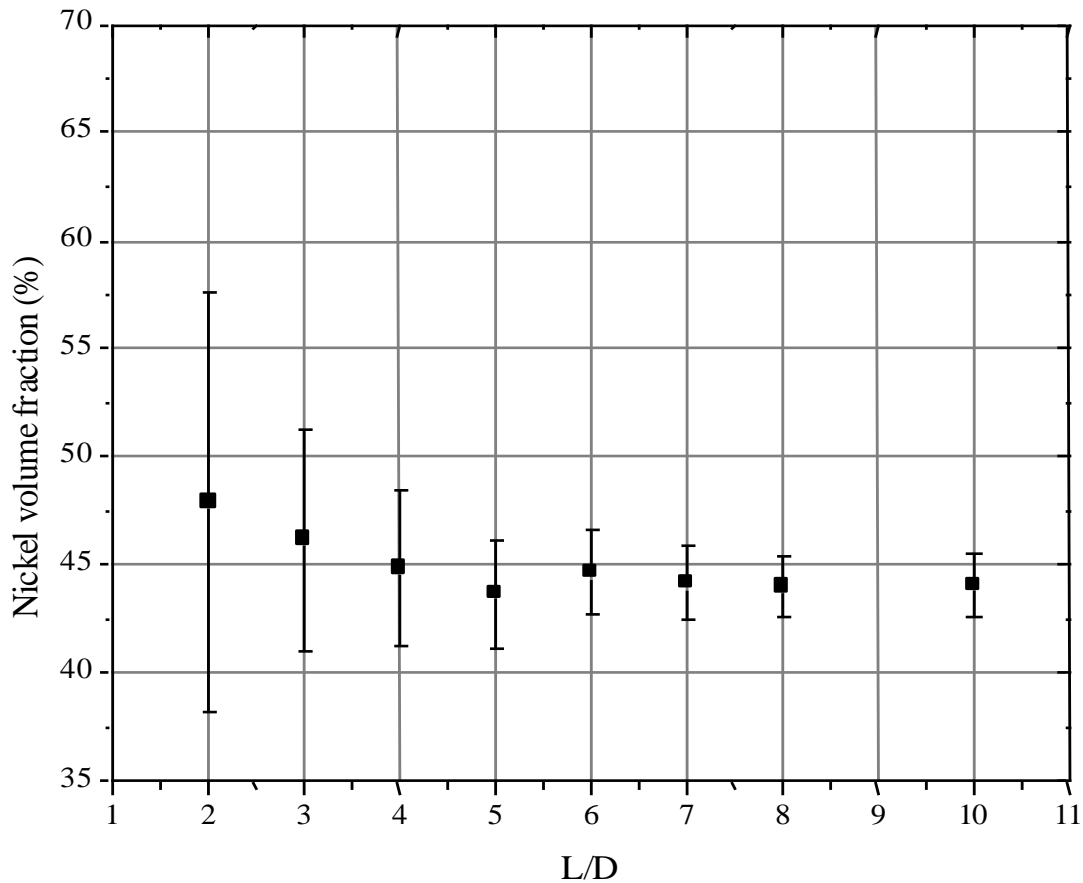
Figure 1 – Nickel volume fraction content (mean and standard deviation) as a function of L/D for families of structures with average composition given by 43.5 vol% Ni, 35 vol% YSZ and 21.5 vol% porosity, with particles of diameter 1 μm.

As the L/D ratio increases, this spread decreases, in turn decreasing the average computed value. The larger effective conductivities for smaller structures are also attributed to the less tortuous paths for charge transport in these structures than in the larger structures. It can indeed be understood that, as the domain size increases, the length of each conducting path between the relevant boundaries increases, as they expand in all three dimensions rather than just one dimension. Figure 3 shows three different microstructures at three different L/D ratios to illustrate the expansion of conducting path networks with increasing domain sizes, with the skeletonized Nickel paths highlighted within each structure. The algorithm to

determine the Nickel paths is a thinning algorithm developed by Zhang and Suen [27], which is well established in the literature [28, 29].
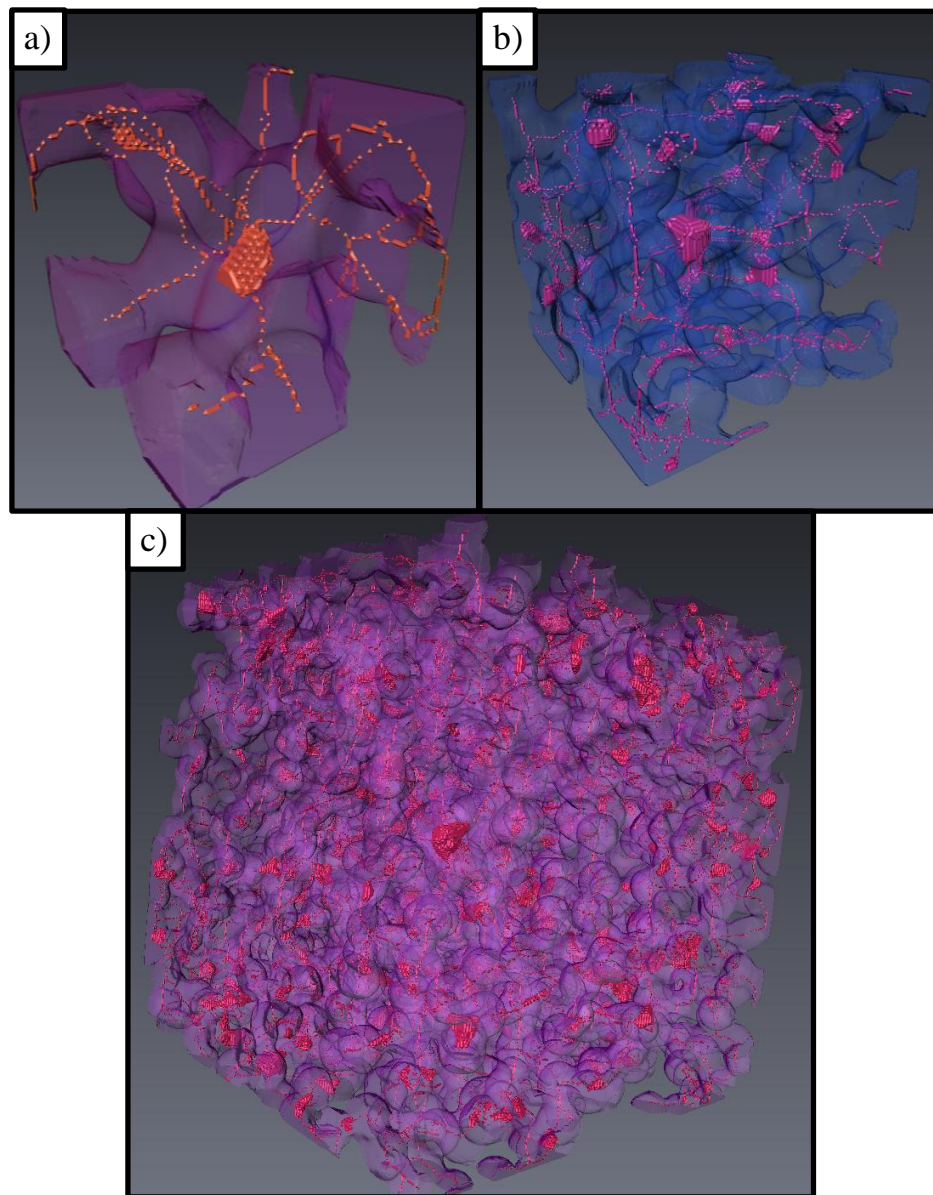

Figure 3 – Graphical representation of sample microstructures at L/D = 2 (a), L/D = 5 (b) and L/D = 10 (c), with the skeletonized paths highlighted in each microstructure.

The structures presented in Figure 3 are characterized by an L/D ratio of 2, 5 and 10, respectively and are comprised of a total of 16.4, 1.46×10^2 and 3.34×10^3 μm of connected paths, respectively. The total connected path length increases exponentially for an increasing domain size.

3. The experimental electrodes

3.1 Experimental preparation of the electrodes and measurement of the effective conductivities

The real microstructures of the Ni/10ScSZ cermet anode films used here were obtained with the electrode sample fabrication method of Somalu *et al.* [30]. A brief description is given here.

Intially, four NiO/10ScSZ anode composite powders with 20, 30, 40 and 50 vol% Ni were prepared by mechanical mixing of NiO and ScSZ (10 mol% Sc_2O_3- 90 mol% ZrO_2) powders. In the preparation of NiO/10ScSZ screen-printing inks, the anode composite powders were mixed with the basic ingredients of solvent (terpineol), dispersant (hypermer KD15) and a binder (ethyl cellulose) before homogenizing them using a triple roll mill (EXAKT 80E, Germany) [30].

All the SOFC anode films were fabricated by screen-printing one of the four NiO/10ScSZ composite inks onto yttria-stabilized-zirconia (YSZ) pellets before sintering at 1250 ^{o}C, 1300 ^{o}C or 1350 ^{o}C for 1 h in a furnace to obtain 12 different samples. After sintering, the anode films were reduced in a mixture of hydrogen (10%) and nitrogen (90%) gas which was humidified at room temperature. The reduction process was carried out at 800 ^{o}C for 2 h. After the reduction process, Ni/10ScSZ anodes with volumetric ratios of Ni to 10ScSZ of 20:80, 30:70, 40:60 and 50:50 were obtained.

The in-plane electronic conductivity of the Ni/10ScSZ anode films was determined by the van der Pauw technique with a 4-point probe connected to an Autolab PGSTAT30 (Metrohm) in a mixture of dry hydrogen (10%) and dry nitrogen (90%) gas at 700 ^{o}C [30].

The gas supply was needed to avoid any oxidation of Ni to NiO in the anode during the conductivity measurements.

3.2. 3D Imaging and Reconstruction

In order to obtain real anode microstructures to be used as an input for a conductivity analysis with the ResNet model, the 3D anode microstructure was probed and captured using FIB-SEM tomography. Before imaging, the anode samples were impregnated with epoxy resin (Specifix20, Struers, UK) under vacuum conditions so that the pores of the anodes could be better distinguished during SEM imaging. The cured samples were mechanically cut and polished to ensure a flat cross-section. The 3D microstructure of the anode samples was imaged using an Auriga (Zeiss) FIB-SEM system. About 500 slice images were obtained from each sample, using a voxel size of 30 nm × 30 nm × 30 nm. Two solid phases were distinguished with an in-lens secondary electron detector. The alignment and segmentation of the images were carried out to reconstruct the 3D electrode microstructure based on intensity boundary values that represented features of interest. Following this step, microstructural parameters that characterize the porous microstructure were quantified, such as volume fractions and the mean particle/pore sizes. Both processes utilized in-house image processing programs and commercially available software (Avizo, FEI, Bordeaux, France). The average particle/pore sizes were quantified with the mean-intercept method (MIL) [31]. A more detailed description of the procedure used for imaging, image processing and quantification can be found elsewhere [11, 17, 24].

The sizes of the reconstructed sample and the values of the parameters described above are summarized in Table 1. Four samples of Ni/10ScSZ sintered at 1350°C were analyzed; the names of the samples – Ni20, Ni30, Ni40 and Ni50 reflect the volume ratios of Ni to 10ScSZ used to manufacture these samples, namely 20:80, 30:70, 40:60 and 50:50, respectively,.

Following the analysis in Section 2, the samples need to be at least 8 times larger than the average particle size used during fabrication to be representative of the entire anode. According to the quantitative microstructural parameters, the maximum average particle size (MIL) for all the microstructures was found to be 1.23 µm in the Ni phase in the Ni50 sample, meaning that a minimum sample size of 9.84 µm × 9.84 µm × 9.84 µm is required for a sample to be representative. As can be seen in Table 1, the samples measured were larger than this minimum sample size. The volume ratios of Ni to 10ScSZ were 19.3:80.7, 29.7:70.3, 41.4:58.6 and 50.7:49.3, respectively, and are thus similar to the volume ratios used for manufacture, as described in Section 3.1. This indicates that the reconstructed volume was large enough to be representative of the electrode as a whole.

Table 1

The sample sizes and the quantified parameters of the reconstructed electrode microstructures

		Ni20	Ni30	Ni40	Ni50
Sample size [µm]	X	17.6	16.2	18.6	17.8
	Y	19.4	11.7	12.0	14.8
	Z	14.9	14.0	13.5	11.0
Volume fraction [%]	Ni	16.1	20.9	26.3	30.6
	ScSZ	67.4	49.5	37.2	29.8
	Pore	16.6	29.7	36.4	39.7
Average particle/pore size [µm]	Ni	0.765	0.854	1.02	1.23
	ScSZ	0.837	0.836	0.810	0.725
	Pore	0.622	0.794	0.938	1.02

4. Validation of the ResNet model

The effective conductivity of each reconstructed microstructure was computed using the ResNet model. These were then aggregated into larger volumes (the so-called VOF elements) at the level of 5^3 voxels per VOF element. Figure 4 shows the effective conductivities experimentally measured on the Ni/10ScSZ electrodes of different Ni content, compared to the effective conductivities computed by the ResNet model on the four reconstructed electrodes (corresponding to the electrodes sintered at 1350^oC). Also presented in Figure 4 are the electronic conductivities of a set of synthetic structures, as computed by the ResNet model. These synthetic structures were generated with similar compositions to those fabricated by Somalu *et al.* [30] and subsequently reconstructed. The particle diameter was also set to match those used by Somalu *et al.* in their real anodes [30], namely 0.765μm for the Ni20 sample, 0.854 μm for the Ni30 sample, 1.02 μm for the Ni40 sample, and 1.23 μm for the Ni50 sample (post-enlargment). 10ScSZ was used for the ionic phase and attributed an ionic conductivity of 0.11 S/cm [32]. Finally, a last dataset is presented in order to compare the output from the ResNet model to the volume-averaged approach by Golbert *et al.* [18]. This approach is applied to a theoretical set of synthetic structures with increasing Nickel contents in the solid phase. This dataset was obtained by multiplying the conductivity of pure Ni by the volume fraction content of Ni in each VOF element and applying the ResNet model to compute the effective conductivity for the network of the VOF elements.
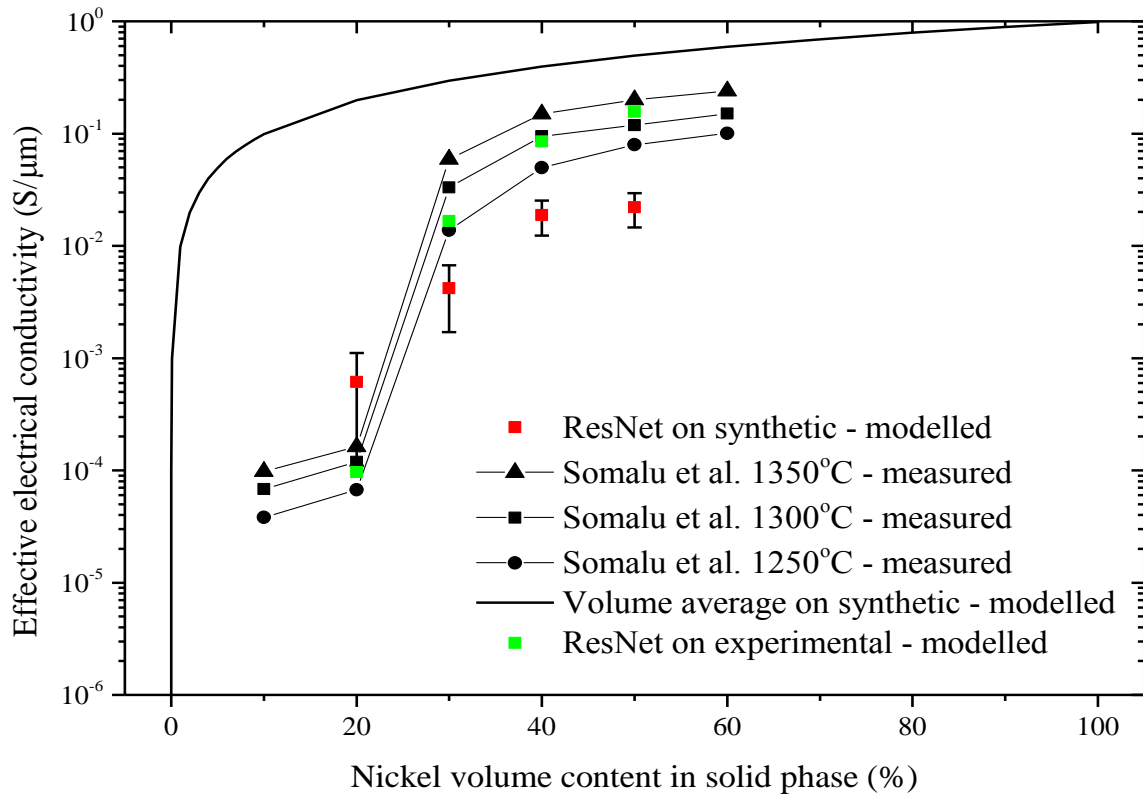
Figure 4 – Variation of effective electronic conductivity of Ni/10ScSZ anode films measured at 700°C as a function of Ni content in the solid phase, compared to calculated values based on the 3D imaging of the same anode films sintered at 1350°C, and values calculated from synthetically generated structures with identical compositions. All conductivities presented are computed in the x-direction.

As shown in Fig. 4, there is good agreement between the experimentally measured effective conductivities of the Ni/10ScSZ anode films and those computed by the ResNet model using the reconstructed microstructures from the same electrodes. The agreement is seen for a range of samples with different Ni contents. Both the experimental measurement and ResNet prediction show a steep increase in electronic conductivity at around 30 vol% Ni content, found to be the percolation threshold for a Ni cermet to have electronic conducting pathways throughout the electrode. This correlates well with values reported in experimental investigations by Somalu *et al.* [30] and Dees et al. [33]. The results also show a large

variation in the conductivity values as the percolation threshold is approached, highlighting the sensitivity of the conductivity to the local microstructure when the Ni content of the electrode is close to the percolation limit. The experimentally-derived and model-predicted effective conductivities are found to have values of the same order of magnitude. The small discrepancy that is observed may be attributed to errors in experimental measurement of the effective conductivies, and errors arising from the image segmentation and reconstruction techniques used to obtain the 3D microstructures [17]. Nevertheless, the good agreement between the experimental and model-predicted effective conductivities supports the use of ResNet model for the prediction of effective conductivities for SOFC electrodes, as well as giving confidence in the 3D imaging techniques and subsequent image processing methodologies.

The application of the ResNet model to the synthetic electrode structures yields an increase of effective electronic conductivity as the Ni volume content increases. Effective electronic conductivities predicted by the ResNet model on synthetic structures are found to be lower than the experimentally measured values past the percolation thershold, with the closest agreements occurring at Ni contents under the percolation threshold. A steadier increase in effective electronic conductivity across this threshold is observed, and families of electrodes characterized by a 40% and 50% Nickel content only differ in effective electronic conductivity by 14.5%. This is due to the fact that the absolute Nickel content in both of these families of structures varies by as little as 4.1%.

The variation of effective electronic conductivity of families of synthetic microstructures will now be investigated with regards to increasing Nickel content in the solid phase, this time at a constant porosity of 41.2.% and uniform particle size of 1μm.
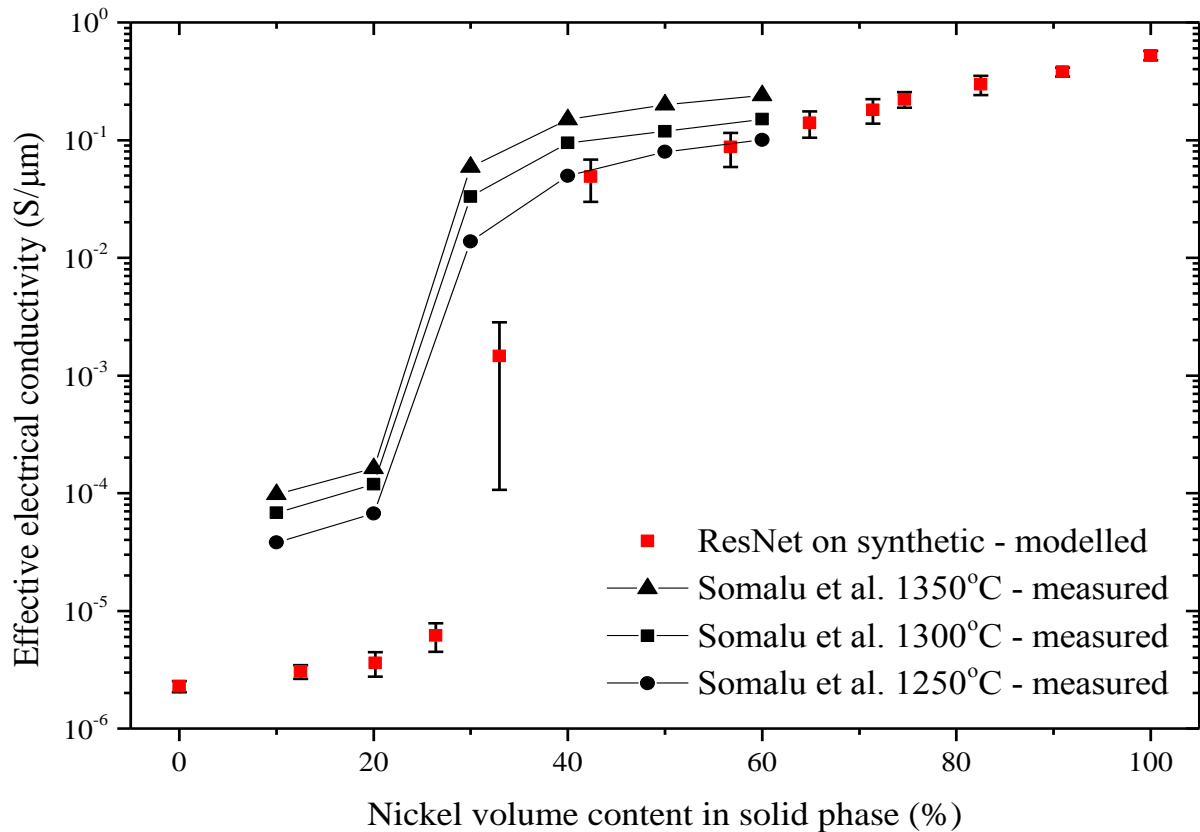
Figure 5 – Variation of effective electronic conductivity of Ni/10ScSZ anode films measured at 700^oC as a function of Ni content in the solid phase, compared to values calculated from synthetically generated structures with a constant porosity of 41.2%. All conductivities presented are computed in the x-direction.

The application of the ResNet model to the synthetic electrode structures yields a similar trend as the experimental data, with an increase of effective electronic conductivity as the Ni volume content increases. Effective electronic conductivities predicted by the ResNet model on synthetic structures are found to be lower than the experimentally measured values, with the closest agreements occurring at Ni contents above the percolation threshold.

The results illustrated in Figures 4 and 5 highlight the importance of correctly modeling the sintering process used for fabricating SOFC electrodes, which is not captured in the algorithm developed by Golbert *et al.* [18] for the generation of the synthetic structures. Also, it is

understood that in real electrodes, particles are not perfectly spherical; in contrast, the synthetic microstructures are generated using spherical particles, which undergo an expansion process and become cut spheres. All these factors can contribute to the difference between the effective conductivities predicted by the ResNet model on experimental and synthetic microstructures.

In all cases, the volume-averaged approach used by Golbert *et al.* [18] is found to yield a gross over-estimation of the effective conductivity at all considered volume fractions, and does not capture the percolation threshold.

5. Application of the ResNet model to the prediction of electrochemical performance

In the final part of this study, the ResNet model is integrated with the VOF method to predict the electrochemical performance of SOFC electrodes. This makes it possible to assess the impact of errors in the electronic conductivity on the predicted electrochemical performance. The effect of effective conductivity on current generation is investigated first for the electronic nickel phase, and then for the ionic YSZ phase, through the application of the ResNet model to calculate the local effective conductivity of the relevant phase.

The synthetic structures generated for the analysis presented in Figure 1 were used to model electrochemical performance. The microstructures were first discretized into voxels; 20 voxels per particle were used to ensure a sufficient discretization and high solution accuracy. This discretization was followed by the aggregation of voxels into VOF elements, at a level of 5^3 voxels in each VOF element; this was determined to be the optimum resolution in previous work, offering a good balance between accuracy and computational cost [23]. The local effective conductivity of each VOF element was computed using the ResNet model instead of the volume-fraction averaged conductivity. The resulting model of the anode

structure and properties was then used in the VOF method to predict electrochemical performance. The combination of both models is referred to as the combined ResNet-VOF model.
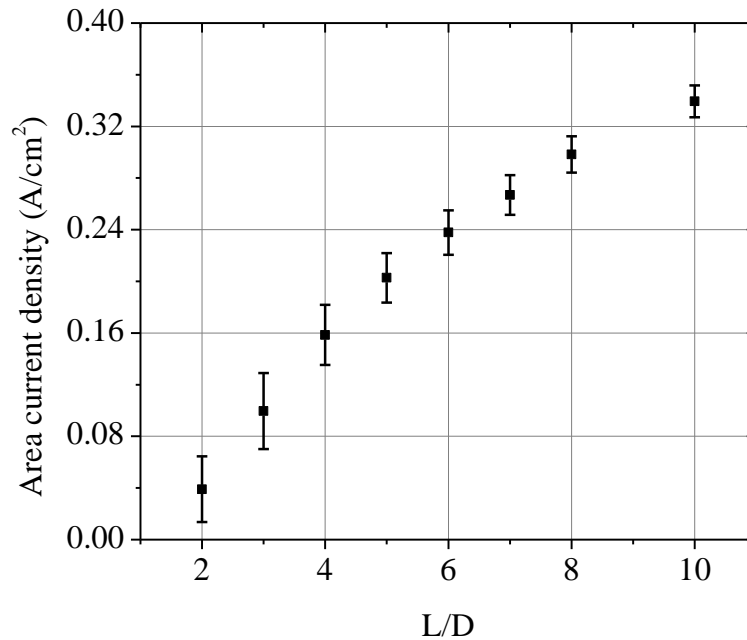

Figure 6 – Calculated area-specific current density at an overpotential of 50 mV as a function of L/D for families of structures with a 43.5 vol% Ni, 35 vol% YSZ and 21.5 vol% porosity. The diameter of particles is fixed at 1 μm.

Figure 6 shows the area current density predicted by the combined ResNet-VOF model when the ResNet model is applied to the electronic conducting phase to calculate the effective conductivity of each VOF element. The area current density for the same set of microstructures was also computed using the original VOF model [18], in which the volume-fraction averaged conductivity is used for each VOF element. A very small difference was found between the two sets of results, of the order of 0.001% for the average and standard deviation. Due to the small difference observed, the results are not plotted on Figure 6. The good agreement indicates that the use of the ResNet-VOF model to include the local electronic conductivity has no significant impact on predicted current density generation for

the range of effective conductivites considered, which vary from 1.19 S/μm at L/D = 2 to 0.63 S/μm at L/D = 10 when using the ResNet model and a constant value of 0.516 S/μm when using the volume-averaged model. Note that the Ni composition of the families of structures considered is 43.5 vol%, which is well above the percolation threshold reported earlier, meaning that a large portion of the microstructure is occupied by the electronically conducting phase. The abundance of charge-carrying paths, together with the high electronic conductivity of Ni, ensures that there is little difference in the effective conductivites computed from the two models. This suggests that, under the conditions examined, i.e., at 800 °C and at an overpotential of 50 mV, and with a well percolated (and therefore conducting) Ni microstructure, the effective conductivity of the Ni phase of an SOFC anode has little or no impact on current generation. In other words, electron transport is not rate-limiting.
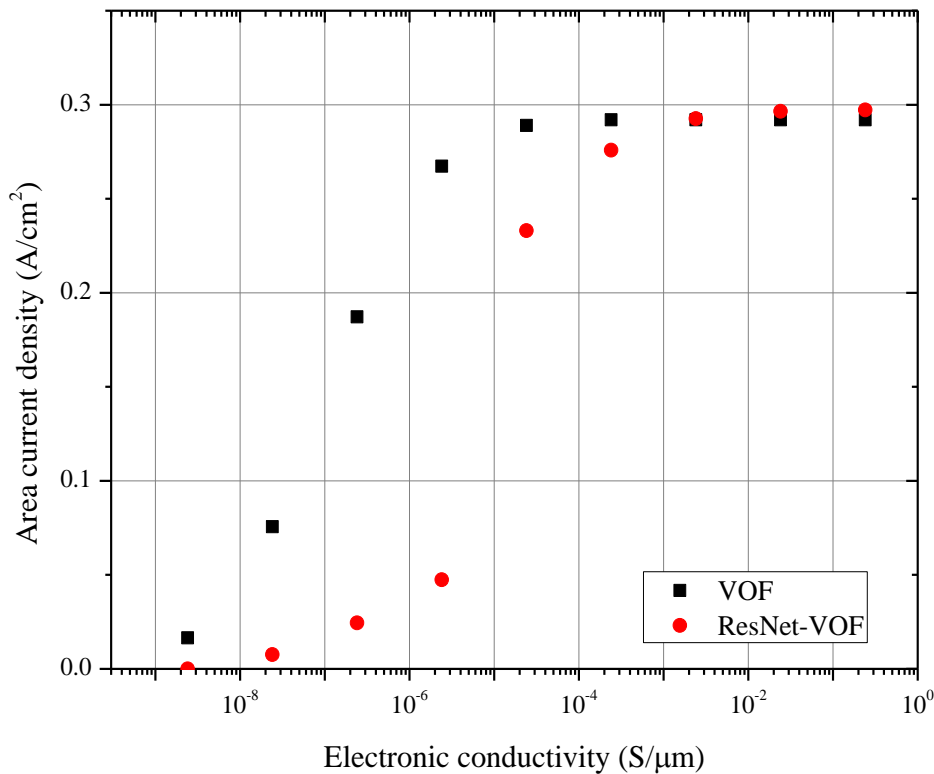
Figure 7 – Calculated area-specific current density as a function of electronic conductivity for a sample structure with L/D = 8, a 43.5 vol% 'electronic phase', 35 vol% YSZ, 21.5 vol% porosity, and particles of diameter 1 μm. All conductivities presented are computed in the x-direction.

Much lower electronic conductivities, however, are expected to inhibit the anode's ability to transfer current from the reaction sites to the current collector. A sensitivity analysis was carried out to explore the effects of the electronic conductivity on current generation. Figure 7 shows the effect of varying the conductivity of the electronic phase over a wide range of 1.0×10^{-9} S/μm to 1.0×10^{1} S/μm for a sample synthetic structure with L/D=8. Both the ResNet-VOF model and the VOF model were used to determine how the use of each model impacts the predicted electrochemical performance of model structures while varying the conductivity of the electronic phase. In both cases, it is the electronic conductivity of the nominal 'nickel' phase that is varied to ensure the conservation of local differences in electronic conductivities. It can be seen from Fig.7 that when the conductivity of the electronic phase is larger than 10^{-3} S/μm, the area current density predicted using the combined ResNet-VOF model and that predicted by the VOF model are in very good agreement; when the conductivity of the electronic phase is smaller than 10^{-3} S/μm, there are indeed visible differences in the area current density predicted from the two models. In operation, Ni has an electronic conductivity that varies between 2.00 S/μm at 1000 °C and 2.86 S/μm at 500 °C [34], which is 3 orders of magnitude larger than the electronic conductivity that would start to limit current generation. This analysis shows that, for percolated structures, the effective conductivity of SOFC anodes under standard operating conditions is a parameter that has a relatively small effect on the performance of these electrodes. The analysis also demonstrates that using the original VOF model is a suitable approximation when predicting the electrochemical performance of Ni cermet anodes, if the Ni phase is properly percolated. For

cathode materials where the electronic phase has a lower conductivity, the use of the combined ResNet-VOF model can be expected to provide more accurate predictions of current generation.

From Figure 7, it can also be seen that at low phase conductivity ($<10^{-3}$ S/μm), the predicted electrochemical performance using the ResNet-VOF model becomes sensitive to the phase conductivity value. Therefore it is anticipated that the use of the ResNet model to describe the local ionic conductivity can give more accurate electrochemical performance prediction, since the ionic phase in SOFC electrodes normally has a much lower conductivity than 10^{-3} S/μm. The ResNet model was hence used to compute the effective ionic conductivity of the same synthetic microstructures as in Figure 4, for use in the VOF model to predict electrochemical performance. Figure 8 shows the area-specific current density generated for a family of microstructures using both the combined ResNet-VOF model and the VOF model. It can be seen from Figure 8 that the difference in the current densities computed by the two models is not negligible; the combined ResNet-VOF model predicts lower area-specific current densities. It is evident that the predicted current densities are sensitive to the local effective conductivity of the ionic phase. Therefore, it is important that the local effective conductivity in each VOF element is described by the ResNet model, and the combined ResNet-VOF model should be used to predict electrochemical performance. To better understand this sensitivity, an analysis of the effect of varying the ionic conductivity when using the VOF model and the ResNet-VOF model is presented in Figure 9, for a sample synthetic structure.
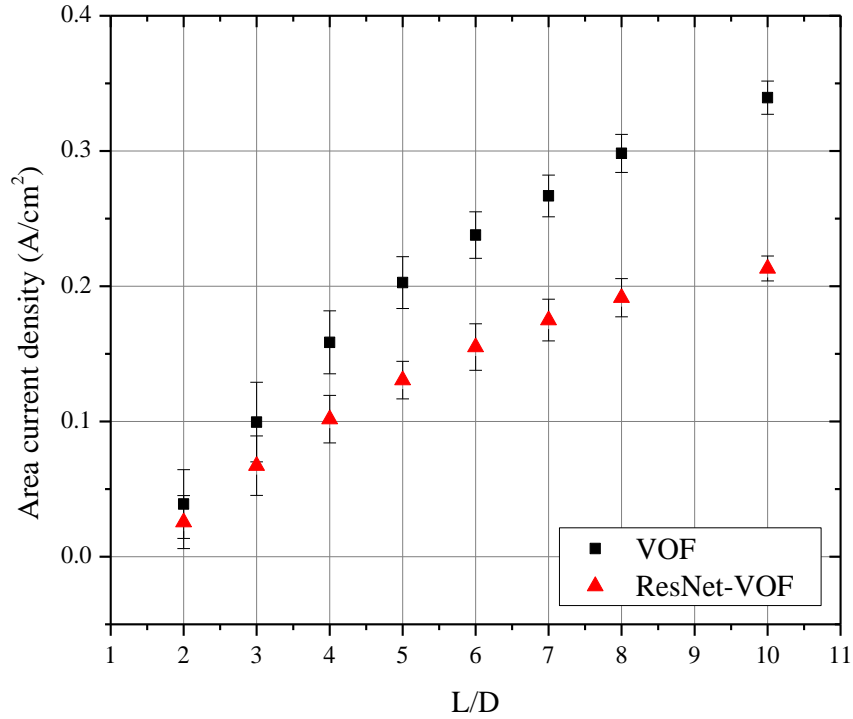
Figure 8 – Calculated area-specific current density (mean and standard deviation) as a function of L/D for families of structures with a 43.5 vol% Ni, 35vol% YSZ and 21.5 vol% porosity with particles of diameter 1 μm at an overpotential of 50mV. The squares represent the results of the VOF model using volume fraction averaged ionic conductivities. The triangles are the result of the ResNet-VOF model based on local effective ionic conductivities.
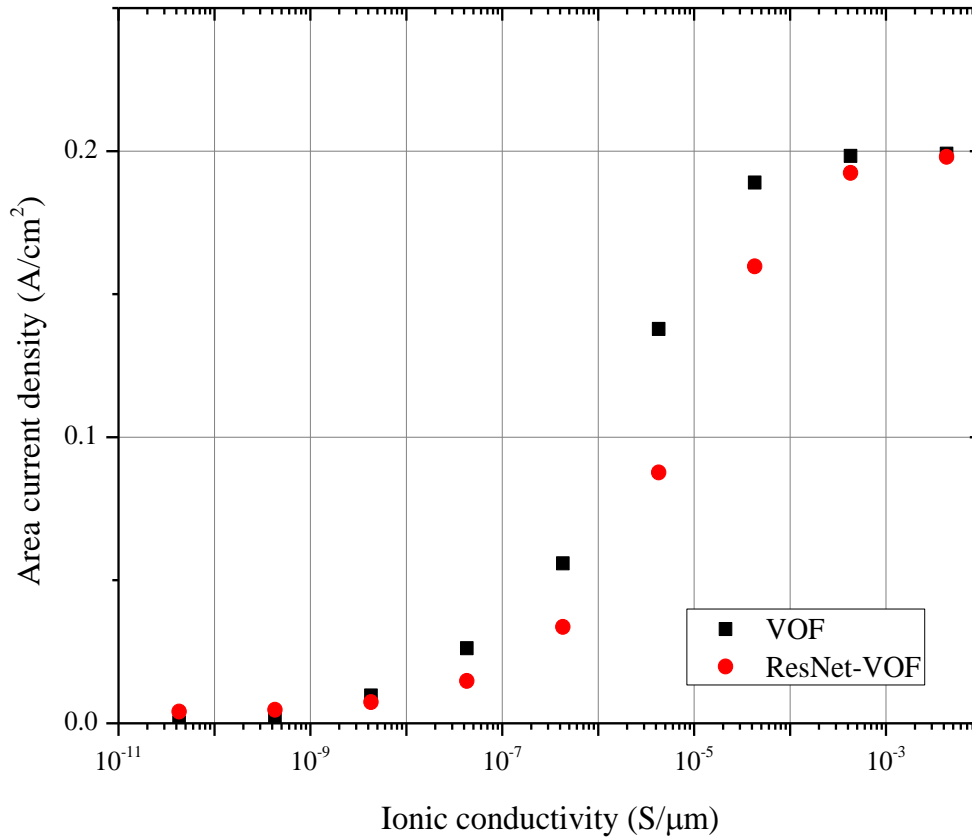
Figure 9 – Calculated area-specific current density as a function of ionic conductivity for a sample synthetic structure with an L/D ratio of 8, a 43.5% volume content of Ni, 35% volume content of YSZ, 21.5% porosity and particles of diameter 1 μm. All conductivities presented are computed in the x-direction.

The ionic conductivity of the YSZ phase in the VOF model at 800 °C is set to be 4.28×10^{-6} S/μm [35]. Using both the ResNet and the volume-average approach for conductivity analysis, the VOF model shows that current generation is sensitive to ionic conductivity values lower than 10^{-3} S/μm. Current densities are seen to steadily drop until ionic conductivity values reach around 10^{-9} S/μm, meaning that conductivity variations between these two boundaries have a direct impact on the current generation capabilities of these synthetic SOFC microstructures. Poor ionic conductivities are indeed understood to impede

the transport of ions to and from reaction sites which slows down the reaction rate and decreases the amount of current generated.

From the results shown above, we can conclude that, when predicting electrochemical performance, it is important to use the ResNet model to give a detailed description of the local ionic conducitivity. It is however good enough to use the volume-average approach for the electronic effective conductivity if the structure is well percolated, mainly because the electronic conductivity is then much bigger than 10^{-3} S/μm and its variation under SOFC operating conditions has a negligible effect on the electrochemical performance.

6. Conclusion

A resistor network (ResNet) model developed to predict the effective conductivity of the SOFC electrodes was applied to real electrodes. First, in order to ensure that the electrode microstructure samples considered were large enough to represent the entire electrode, an analysis on synthetic microstructures was carried out to find the representative sample size. For this analysis, a series of electode microstructures was generated in cubic boxes of varying length L using particles of diameter D = 1 μm. A box with L/D ratio of 8 was determined to be sufficient for electrode samples to be representative of the whole electrode microstructure in terms of effective conductivity.

The 3D microstructures of several SOFC Ni/10ScSZ anodes were charaterized and reconstructed using the FIB-SEM technique, and input to the ResNet model to predict the effective conductivities. The ResNet model was validated by comparing the predicted effective electronic conductivities against the experimentally measured values based on the same SOFC anodes. The effective electronic conductivities of four experimental Ni/10ScSZ anodes with varying Ni to ScSZ ratios predicted using the ResNet model. Good agreement

was found between the experimentally-measured effective conductivities and those computed by the ResNet model on microstructures taken from the same electrodes, sintered at 1350°C. This enabled the validation of the ResNet model and supports the use of the ResNet model to predict the effective conductivity of SOFC electrodes.

The ResNet model was then incorporated into the electrochemical model based on the VOF method to take into account the local conductivity of the microstructure for the prediction of electrochemical performance of SOFC electrodes, resulting in the so-called ResNet-VOF model. The results showed that, when the bulk phase conductivity is bigger than 10^{-3} S/μm, the local conductivity does not affect the electrochemical performance and thus the VOF method alone, which uses a volume-averaged approach to calculate the effective conductivity, is adequate to predict electrode performance. This means that for the Ni phase, which has an bulk electronic conductivity much bigger than 10^{-3} S/μm under operating conditions, it is sufficient to use the volume-average approach to predict electrochemical performance without including local electronic conducivity.

It was however established that the electrochemical performance was sensitive to the local ionic conductivity within the electrode, as the ionic conductivity of the oxide ion conducting phase under normal SOFC operation is much smaller than 10^{-3} S/μm. It is thus important that the local ionic conductivity is described accurately. Therefore use of the ResNet model is recommended to predict the local effective ionic conductivity, to enable a more accurate prediction of the electrochemical performance. Finally it was found that L/D > 10 is required for accurate electrochemical performance simulations.

The availability of a validated predictive model such as ResNet-VOF provides a new tool for the understanding and design of electrode microstructures. In combination with improved imaging capabilities, it can be used to gain insights into the underlying physical phenomena

that affect performance. The usefulness of such a model would be further enhanced if it could be combined with more realistic algorithms for the generation of synthetic structures, thereby providing more quantitative support for electrode design.

References

[1]   D. Chen, Z. Lin, H. Zhu, R. J. Kee, Journal of Power Sources 191 (2009) 240–252.

[2]   A. Bertei, C. Nicolella, Journal of Power Sources 196 (2011) 9429–9436.

[3]   A. Bertei, A.S.Thorel, W.G.Bessler, C.Nicolella, Chemical Engineering Science 68 (2012) 606–616.

[4]   J. Abel, A. A. Kornyshev, and W. Lehnert, J. Electrochem. Soc, 144 (1997) 4253-4259

[5]   L.C.R. Schneider, C.L. Martin, Y. Bultel, D. Bouvard, E. Siebert, Electrochimica Acta 52 (2006) 314–324

[6]   Yan Ji, Kun Yuan, J.N. Chung, Journal of Power Sources 165 (2007) 774–785

[7]   A. Abbaspour, J.-L. Luo, K. Nandakumar, Electrochimica Acta 55 (2010) 3944–3950

[8]   D. Gostovic, J. R. Smith, D. P. Kundinger, K. S. Jones, and E. D. Wachsman, Electrochemical and Solid-State Letters, 10 (2007) B214-B217.

[9]   Y. Suzue, N. Shikazono, N. Kasagi, Journal of Power Sources 184 (2008) 52–59.

[10]   P.R. Shearing, J. Gelb, N.P. Brandon, Journal of the European Ceramic Society 30 (2010), 1809-1814.

[11]   M. Kishimoto, H. Iwai, M. Saito, H. Yoshida, J. Power Sources 196 (2011) 4555.

[12]   J. R. Wilson, J. Scott Cronin and S. A. Barnett, Scripta Materialia 65 (2011) 67–72.

[13]   N. S. K. Gunda, H.-W. Choi, A.Berson, B. Kenney, K. Karan, J.G. Pharoah, S.K. Mitra, Journal of Power Sources 196 (2011) 3592–3603.

[14]   M. E.Lynch, D. Ding, W. M.Harris, J. J.Lombardo, G. J.Nelson, W. K.S.Chiu, M. Liu, Nano Energy 2 (2013), 105–115.

[15]   N. Shikazono, D. Kanno, K. Matsuzaki, H. Teshima, S. Sumino, N. Kasagi, Journal of The Electrochemical Society 157 (2010) B665.

[16]   M. Kishimoto, H. Iwai, M. Saito, H. Yoshida, Journal of Electrochemical Society, 159 (2012) B315-B323.

[17]   M. Kishimoto, H. Iwai, K. Miyawaki, M. Saito, H. Yoshida, Journal of Power Sources 223 (2013) 268-276.

[18]   J. Golbert, C. S. Adjiman, N. P. Brandon, Ind Eng Chem Res 47(2008) 7693-7699.

[19]   P.R. Shearing, Q. Cai, J.I. Golbert, V. Yufit, C.S. Adjiman, N.P. Brandon, Journal of Power Sources 195 (2010), 4804-4810.

[20]   Q. Cai, C. S. Adjiman, N. P. Brandon, Electrochimica Acta 56 (2011) 5804-5814.

[21]   Q. Cai, C. S. Adjiman, N. P. Brandon, Electrochimica Acta 56 (2011) 10809-10819.

[22]   K. Rhazaoui, Q. Cai, C.S. Adjiman, N.P. Brandon, Chem. Eng. Sci. 99 (2013) 161-170.

[23]   K. Rhazaoui, Q. Cai, C.S. Adjiman, N. P. Brandon, Chem. Eng. Sci. 116 (2014) 781-792.

[24]   H. Iwai, N. Shikazono, T. Matsui, H. Teshima, M. Kishimoto, R. Kishida, D. Hayashi, K. Matsuzaki, D. Kanno, M. Saito, H. Muroyama, K. Eguchi, N. Kasagi, H. Yoshida, Journal of Power Sources 195 (2010) 955-961.

[25]   P.R. Shearing, J. Gelb, J. Yi, W.-K. Lee, M. Drakopolous, N.P. Brandon, Electrochemistry Communications, 12 (2010) 1021‑1024.

[26]   H.-W. Choi, A. Berson1, J. G. Pharoah, S. B. Beale, Proceedings of the Institution of Mechanical Engineers, Part A: Journal of Power and Energy 225 (2011) 183-197.

[27]   T. Y. Zhang, C. Y. Suen, Communications of the ACM 27 (1984) 236-239.

[28]   L. Lam, S-W Lee, Institute of Electrical and Electronics Engineers 14 (1992) 869-885.

[29]   P. S. P. Wang, Y. Y. Zhang, Computers, Institute of Electrical and Electronics Engineers 38 (1989) 741-745.

[30]   M. R. Somalu, V. Yufit, D. Cumming, E. Lorente, N. P. Brandon, International Journal of Hydrogen Energy 36 (2011) 5557-5566.

[31]   D. Simwonis, F. Tietz, D. Stöver. Solid State Ionics 132 (2000) 241-251.

[32]   Y. Mizutani, M. Kawai, K. Nomura, Y. Nakamura, Electrochemical Society Proceedings 99 (1999) 185-189.

[33]   D. W. Dees, T. D. Claar, T. E. Easler, D. C. Fee, F. C. Mrazek, Journal of the Electrochemical Society 134 (1987) 2141-2146.

[34]   M. Yousuf, P.C. Sahu, K.G. Rajan, Physical Review B 34 (1986) 8086-8100.

[35]   N. M. Sammes, Z. Cai, Solid State Ionics 100 (1997) 39-44.

[36]   F. Tariq, M. Kishimoto, V. Yufit, G. Cui, M. Somalu, N.P. Brandon, J. European Ceramic Soc., 34 (2014) 3755-3761.